Luminescent Solar Concentrators based on Renewable Polyester Matrices

Tristan A. Geervliet,[a] Ionela Gavrila,[a] Giuseppe Iasilli,[b] Francesco Picchioni,[a] Andrea Pucci[b,]*

[a]Department of Chemical Engineering/Product Technology, ENTEG, University of Groningen, Nijenborgh 4, 9747AG, Groningen, The Netherlands
[b]Department of Chemistry and Industrial Chemistry, University of Pisa, Via Moruzzi 13, 56124 Pisa, Italy; Email: andrea.pucci@unipi.it

*Corresponding author:

Prof. Andrea Pucci
Department of Chemistry and Industrial Chemistry, University of Pisa, Via Moruzzi 13, 56124 Pisa, Italy;
Tel: +39 050 2219270
Email: andrea.pucci@unipi.it

Abstract

This study reports for the first time the use of bio-based alternatives for PMMA as host matrix for luminescent solar concentrators (LSCs). Notably, two types of renewable polyesters were synthesized in varying molar ratios *via* a two-step melt-polycondensation reaction with dibutyl tin oxide as catalyst. The first is a homopolymer of diethyl 2,3:4,5-di-O-methylene galactarate (GxMe) and isosorbide (IGPn) and the second is a random copolymer of GxMe with 1,3-propanediol and dimethyl terephthalate (GTPn). The two polyesters were found to be optically transparent, totally amorphous with a Tg higher than 45 °C and temperature resistance comparable to PMMA. Lumogen Red (LR) and an aggregation-induced emission (AIE) fluorophore, TPETPAFN, were utilized as fluorophores and the derived thin polymer films (25 μm) were found highly homogeneous, especially for those prepared from GTPn, possibly due to the presence of compatibilizing terephthalate units in the matrix composition and the higher molecular weight. The spectroscopic characterization and the optical efficiency determination (η_{opt}) evidenced LSCs performances similar or superior to those collected from LR/PMMA thin films. Noteworthy η_{opt} of 7.7% and 7.1% were recorded for the GTPn-based matrix containing LR and TPETPAFN, respectively, thus definitely supporting the bio-based polyesters as renewable and highly fluorophore-compatible matrices for high performance LSCs.

1. Introduction

The relation between energy consumption and greenhouse gas emissions has been investigated thoroughly and confirmed[1] and the role of the residential sector in global warming has been pointed out to be significant.[2] The building sector accounts for approximately 40% of primary energy consumption in first world countries and 20-30% globally.[3] Energy losses via windows, walls, light, miscellaneous electric loads or plug loads, etc., significantly impact the degree of energy consumption in buildings. The concept of Net Zero-Energy Buildings (NZEBs) is receiving an increasing amount of attention by the scientific community[4] and policy organizations, such as the European Committee.[5] NZEBs are buildings that balance their energy consumption with the production of renewable energy on a yearly basis. Currently, NZEBs are technically feasible for individual houses and small buildings due to rooftop photovoltaic (PV) cells and efficient insulation.[6] However, considering that approximately 7 m^2/kW of peak power is required for NZEBs[7] the mere use of PVs is not worthwhile for larger buildings since they can only be used on rooftops so far. As accessible solution to this problem, luminescent solar concentrators (LSCs) have been the focus of many new studies.[8] LSCs are devices that absorb incoming sunlight, re-emit the light via fluorescence and, subsequently, capture a substantial portion of this re-emitted light that is concentrated at their side, where it can be converted into electricity by photovoltaic (PV) cells. Although the concept of this system is relatively old,[9] more efficient techniques in the field of harvesting solar energy[8a] and the development of more efficient luminescent systems[10] have led to a renaissance in the field. The major advantage of LSCs is that they are less sensitive to the orientation angle than conventional silicon PV cells and less affected by shadowing effects (e.g. clouds), thus making them ideal for the PV integration on the sides of large buildings.[11] Lastly, besides these technical advantages, LSCs are semi-transparent so that they leave the aesthetics of buildings mostly intact.

Typically, LSCs are slabs of transparent material doped with high quantum yield fluorophores. The refractive index of the host materials higher than air allows to trap mostly of the emitted photons by means of total internal reflection. Photons are then collected at the edges of the LSC to produce electric power by PV cells. In conventional LSCs, fluorophores are incorporated in optically

transparent plates or films of polymers characterized by a relatively high Tg, good durability and good transparency, i.e. all factors that are essential to maximize LSCs' optical efficiency.[12] Current state of the art host polymers are commercially available polymethylmethacrylates (PMMA) that are also effective for providing good compatibility with a wide variety of high quantum yield fluorophores. Nevertheless, the oil-based nature of this polymer is a critical drawback for modern urban areas, being the use of solar harvesting systems or devices based on renewable materials also highly desirable. Over the past decades, attention towards bio-based polymers and bio-based platform chemicals has increased tremendously[13] but only a few examples are reported in literature as renewable matrices in LSC composition.[14] Authors efficiently reported the use L-poly(lactic acid) (L-PLA) and cellulose nanocrystals as green alternatives to PMMA for LSCs being characterized by similar refractive index, processability and transparency. Also, biomass offers the advantage of being a source of novel building blocks that can lead to a broader range and even higher performance polymeric materials.[15] For example, isosorbide and furandicarboxylic acid (FDCA) building blocks are currently commercially available examples derived from sugars and are reported in numerous polymer syntheses suitable for engineering thermoplastics.[16] Related to this aspect, the transesterification reaction of acetalised galactarate esters such as dimethyl-2,3:4,5-di-O-isopropylidene-galactarate (GxMe) with 1,6-hexanediol has been recently reported by us as effective in the preparation of bio-based polyesters with targeted characteristics (i.e., molecular weight, dielectric constant and hydrolytic stability).[17]

On this account, we herein report the synthesis of two sugar-based polymers, i.e. a GxMe and isosorbide derived homo-polyester and a copolymer of GxMe with 1,3-propanediol and dimethyl terephthalate, and their utilization as thin film in the preparation of LSC. As fluorophores, Lumogen Red 305 (LR) was utilized as the state of the art dopant in LSCs and their optical efficiencies compared with those of standard PMMA-based solar collectors. The study was also extended to the use of 2,3-bis(4-(phenyl(4-(1,2,2-triphenylvinyl)phenyl)amino)phenyl)fumaronitrile (TPETPAFN) that is an aggregation-induced emission fluorophore,[18] i.e. an important class of emissive materials recently found as promising in high performance LSCs.[19]

2. Experimental part

Materials

1,3-propanediol (>99%), dimethyl terephthalate (>99%), dibutyltin (IV) oxide (DBTO) (98%) were purchased from Sigma-Aldrich and used as received. Diethyl 2,3:4,5-di-O-methylene-galactarate (>99%) was received from Royal Cosun; 1,4:3,6-dianhydrosorbitol (isosorbide) (>98%) was purchased from TCI Chemicals and both used without further purification. Poly(methyl methacrylate) (PMMA, Aldrich, Mw = 350,000 g/mol, acid number <1 mg KOH/g) and Lumogen Red F350 (LR, BASF) were used as received. TPETPAFN was received from AIEgen Biotech Co., Limited (Hong Kong) and used without purification. Optically clear glass slides were prepared by cleaning in 6 M HCl for 12 h, rinsing with water, acetone and 2-propanol and then drying for 8 h at 120 °C.

Polymer synthesis

The protocol used in the present study is adapted from the previously reported synthesis of similar polymer structures. For all polymerizations, the overall mass of the monomers was about 5-6 g.[17]

GxMe-Is homopolymers (IGPn): an equimolar mixture of GxMe and isosorbide together with an amount of 0.5 mol.% of DBTO were brought into a 3-neck cylindrical flask equipped with a magnetic coupling stirrer, a nitrogen gas inlet and a temperature controlled distillation setup. The initial temperature of the reaction was fixed at 140 °C and the mixture was vigorously stirred at 1000 rpm under a constant nitrogen flow. Subsequently, the distillation setup was replaced with a vacuum adapter and high vacuum was applied (0.01 mbar). The progress of the reaction was followed by monitoring the torque values while keeping the temperature constant. The resulting polymers were dissolved in chloroform and precipitated in an excess of diethyl ether. The polymer powder was recovered by vacuum filtration and dried in the vacuum oven until constant weight. About 3.3 g (yield 65%) and 5.9 g (yield 80%) were recovered for IGP2 and IGP5, respectively.

GxMe copolymers (GTPn): a mixture of GxMe (25 mol.%), 1,3-propanediol (50 mol.%) and dimethyl terephthalate (25 mol.%) together with an amount of 0.5 mol.% of DBTO were brought into a 3-neck cylindrical flask equipped with a magnetic coupling stirrer, a nitrogen gas inlet and a temperature controlled distillation setup. The initial temperature of the reaction was fixed at 140 °C

and the mixture was vigorously stirred at 1000 rpm under a low flow of N_2. After 5 hours, high vacuum (0.01-0.05 mbar) was applied for 4 (GTP3) up to 6 (GTP4) more hours before stopping the reaction. Subsequently, the setup was cooled down to room temperature under a stream of N_2. The resulting polymer were dissolved in chloroform and precipitated in an excess of diethyl ether. The polymer powder was recovered by vacuum filtration and dried in the vacuum oven until constant weight. About 4.3 g (yield 85%) and 2.8 g (yield 60%) were recovered for GTP3 and GTP4, respectively.

Preparation of fluorophore/polymer films for LSC

Different fluorophore/polymer thin films were prepared by pouring about 1.2 mL chloroform ($CHCl_3$) solution containing about 60 mg of polymer and the desired amount of fluorophore (i.e., LR or TPETPAFN) to get concentrations in the range of 0.1–1.5 wt.% on 50x50x3 mm cleaned glass (Edmund Optics Ltd BOROFLOAT window 50x50 TS). $CHCl_3$ evaporation was obtained on a warm plate (30 °C) and in a closed environment. The film thickness was measured to be 25±5 µm (Starrett micrometer). For spectroscopic and microscopic investigations, the polymer films were removed after immersion in water and stored in a desiccator.

Equipment and techniques

^{1}H NMR spectra were recorded at room temperature on a Varian Mercury Plus equipment operating at 400 MHz, using samples of approximately 50 mg dissolved in 1 mL of deuterated chloroform. A total of 64 scans were acquired for each sample. Thermogravimetric analyses were performed using a Mettler Toledo TGA/SDTA851 equipment. The measurements were performed on samples of 5-10 mg under a nitrogen flow of 20 mL/min at a heating rate of 10°C/min, within a temperature range of 25–600 °C. Differential Scanning Calorimetry (DSC) were performed on a Perkin Elmer instrument equipped with an autosampler. Samples of polymer of approximately 5 mg were held at 30 °C for 1 minute, after which they were heated until 180 °C and subsequently cooled down to 30 °C (under a nitrogen flow of 20 mL/min). The glass transition temperature Tg was determined from the second heating cycle. Gel permeation chromatography (GPC) was used to determine the molecular weights

and molecular weight dispersion of polymer samples with respect to polystyrene standards. Samples of 3-5 mg were dissolved in 1 mL of chloroform and injected in a four-channel pump Jasco PU-2089 Plus chromatograph, equipped with a Jasco RI 2031 Plus refractometer and a multichannel Jasco UV-2077 Plus UV-Vis detector set at 252 and 360 nm. The flow rate was set at 1 mL min^{-1} at a temperature of 30 °C which was held constant by a Jasco CO 2063 Plus Column Thermostat. A series composed by two Polymer Laboratories columns PLgelTM MIXED D and a PLgelTM precolumn packed with polystyrene was used to perform the analysis (linearity range 100 Da – 400 kDa). Spectrophotometric measurements were performed using a PerkinElmer Lambda 650 spectrometer with temperature control to within ±0.1 °C. Fluorescence spectra in the solid state were measured at room temperature with a Horiba Jobin–Yvon Fluorolog®-3 spectrofluorometer equipped with a 450 W Xenon arc lamp and double-grating excitation and single-grating emission monochromators. The emission quantum yields of the solid samples were obtained by means of a 152 mm diameter "Quanta-φ" integrating sphere, coated with Spectralon®, using as excitation source the 450 W Xenon lamp coupled with a double-grating monochromator for selecting wavelengths. The Quanta-φ apparatus was coupled to the spectrofluorometer by a 1.5 m fiber-optic bundle in a slit-round configuration, 180 fibers; slit-end termination 10 mm O.D. x 50 mm long; round-end termination FR-274; sheath is PVC monocoil. The optical microscope analysis was accomplished on a Reichert Polyvar optical microscope with crossed polarizers.

Optical efficiency measurements of LSCs

A home-built equipment setup was utilized to measure the efficiency of the LSCs. Each fluorophore concentration was tested in triplicate.[20] A sample holder with the photovoltaic (PV) module (IXYS SLMD121H08L mono solar cell 86 x 14 mm: V_{oc} = 5.04 V, I_{sc} = 50.0 mA, FF > 70%, η_{PV} = 22%) is placed 2.5 cm above a scattering layer. The PV cell is masked with black tape to match LSC edge (50 x 3 mm) so that limiting the stray light to negligible levels. Silicon was used to grease the LSC edge. The other three edges of the LSC were covered with a reflective aluminum tape. A solar simulating lamp (ORIEL® LCS-100 solar simulator 94011A S/N: 322, AM1.5G std filter: 69 mW/cm^{-2} at 254 mm) was housed 27.5 cm above the sample. The PV module was connected to a digital

potentiometer (AD5242) controlled via I2C by an Arduino Uno (https://www.arduino.cc) microcontroller using I2C master library. A digital multimeter (KEITHLEY 2010) was connected in series with the circuit, between the PV module and the potentiometer, to collect the current as a function of the external load. Conversely, the voltage was measured by connecting the multimeter in parallel to the digital potentiometer. Arduino Uno controlled the multimeter via SCPI language over RS-232 bus using a TTL to RS-232 converter chip (MAX232). Arduino Uno was connected to pc via USB port and controlled by a Python script. The measurement cycle began with a signal from PC.

3. Results and discussion

Polymer synthesis and characterization

IGPn homopolymers of diethyl 2,3:4,5-di-O-methylene galactarate (GxMe) and isosorbide (IS) and GTPn co-polyesters of GxMe, 1,3-propanediol (PD) and dimethyl terephthalate (DT) (Figure 1) were synthesized via a two-step melt-polycondensation reaction with dibutyl tin oxide as catalyst according to the recent literature.[17] In both syntheses, ethanol was captured as side product. Transesterification was performed under low nitrogen flow at about 140 °C for as long as the viscosity increased. Subsequently, polycondensation reactions were performed at similar temperature as the transesterifications in order to minimize the decomposition of thermally sensitive sugar compounds, and under vacuum to facilitate the removal of volatile by-products.

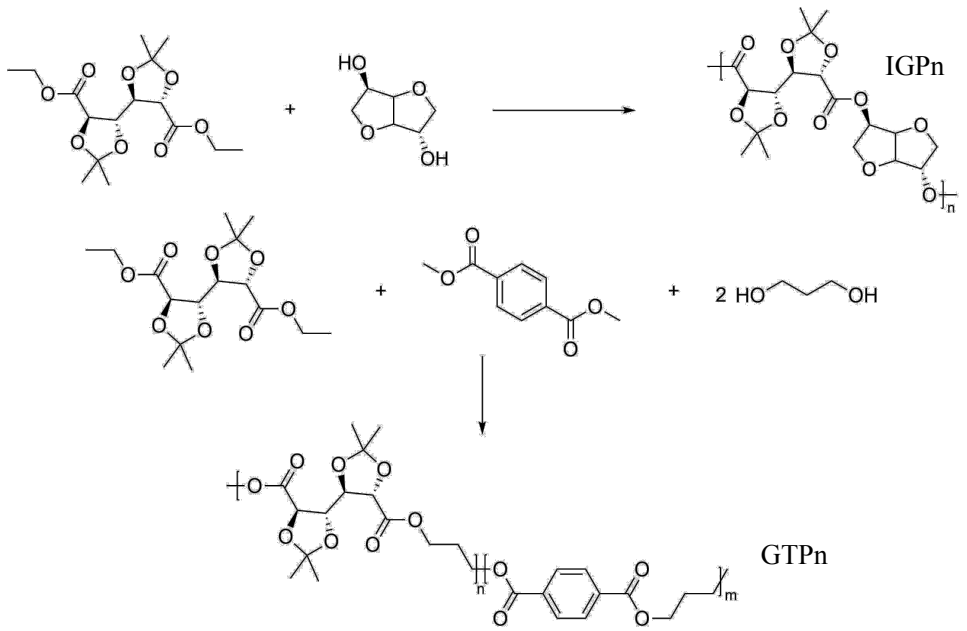

Figure 1. Synthesis of IGPn homo-polyesters and GTPn copolymers

The composition of the polymers was determined by ^{1}H NMR (Figures S1-S4) and the molecular weights and molecular weight distributions were estimated by GPC (see supporting information) (Table 1).

Table 1. Overview composition and M_w of the polymer samples used in the study

Entry	Feed composition (mol.%)				Polymer composition (mol.%)				M_w (g/mol)	M_w/M_n
	GxMe	IS	PD	DT	GxMe	IS	PD	DT		
IGP2	50	50	-	-	58	42	-	-	3500	1.6
IGP5	50	50	-	-	51	49	-	-	3000	1.3
GTP3	25	-	50	25	27	-	50	23	20000	1.6
GTP4	25	-	50	25	28	-	50	22	44000	1.6

For IGPn homo-polyesters, which were obtained from the reaction between GxMe and isosorbide, a slow reactivity of the diol was found. This feature was attributed to the different possible orientation of isosorbide hydroxyl functionalities with the endo-OH group being significantly less reactive than the exo-OH.[16a, 21] Accordingly, homo-polyesters with low weight average molecular weights of 3000-3500 g/mol were gathered after 5-6 hours of reaction. Conversely, for the case of GTPn copolymers, which were obtained from the reaction between GxMe, 1,3-propanediol and dimethyl terephthalate, the conversion to the polymer proved to be higher and two different samples of similar composition were successfully prepared with average M_w between 20000 g/mol (GTP3) and 44000 g/mol (GTP4) (Table 1), according to the different reaction time (4 and 6 hours of vacuum, respectively).

As far as the final applications in LSCs is concerned, the utilized polymers should be totally amorphous, colorless and with a Tg higher than room temperature, e.g. > 45 °C.[12] UV-Vis-NIR experiments revealed that the polymers are mostly transparent in the visible range and with limited light absorption in the Vis-NIR region up to 2500 nm (Figure S5). DSC measurements (Figure S6) indicated that both IGPn and GTPn are amorphous with a Tg according to the required specifications (Table 2). The IGP2 and IGP5 samples showed the highest Tg of 60 °C and 70 °C compared to 45 °C and 48 °C for the GTP3 and GTP4 terephthalate copolymers, thus indicating a negligible influence of the molecular weight in the thermal properties of the materials. Notably, this results is noteworthy

considering the low M_w range of the isosorbide-based homo-polyesters. In terms of thermal stability, all GxMe polyesters are comparable to PMMA (Table 2). Onset degradation temperatures (5% weight loss, $T_{5\%}$) were found higher than 290-300 °C, thus making IGPn and GTPn suitable for LSCs application.

Table 2. Thermal characteristics of the prepared polymers

Entry	T_g (°C)	$T_{5\%}$ (°C)	T_d (°C)
IGP2	75	300	358
IGP5	65	293	371
GTP3	44	328	372
GTP4	46	-	-
PMMA	100	252	400

Optical properties and morphology of polymer films

IGPn and GTPn films with a thickness of 25 ± 5 μm (Starrett micrometer) were prepared by pouring about 1.2 mL chloroform ($CHCl_3$) solution containing about 60 mg of the polymer and the desired amount of LR or TPETPAFN (Figure 2). Red emitting fluorophores were selected since they well-match with the external quantum efficiency of the Si-based PV module used in the photovoltaic experiments of this work.[22]

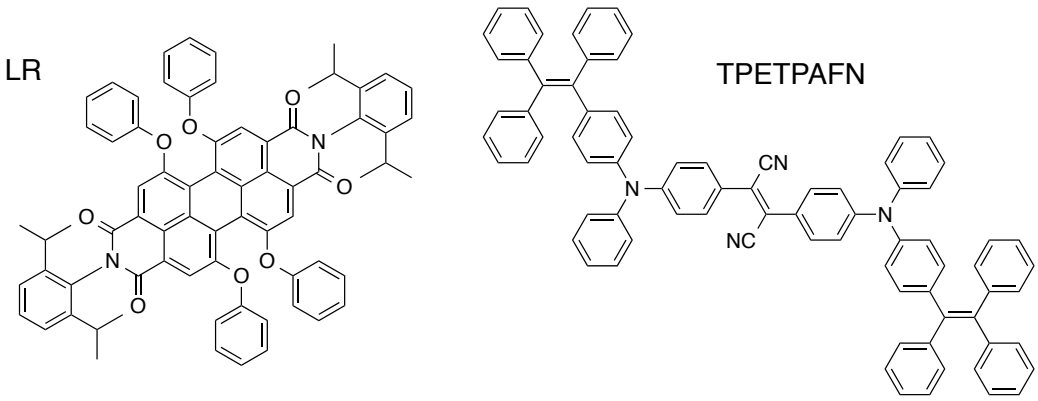

Figure 2. Chemical structures of the fluorophores investigated in this work

In Figure 3a, the absorption and emission characteristics of LR/IGP2 films are reported. LR shows molecular absorption maximum at about 570 nm with a broad absorption band from 410-550 nm,

which result mostly similar to those recorded in PMMA films.[22] Notably, no evident absorption bands attributed to the formation of LR aggregates are observed and absorbance intensities increase regularly with fluorophore content, and without leveling off at the highest concentration (i.e., 1.4 wt.%).

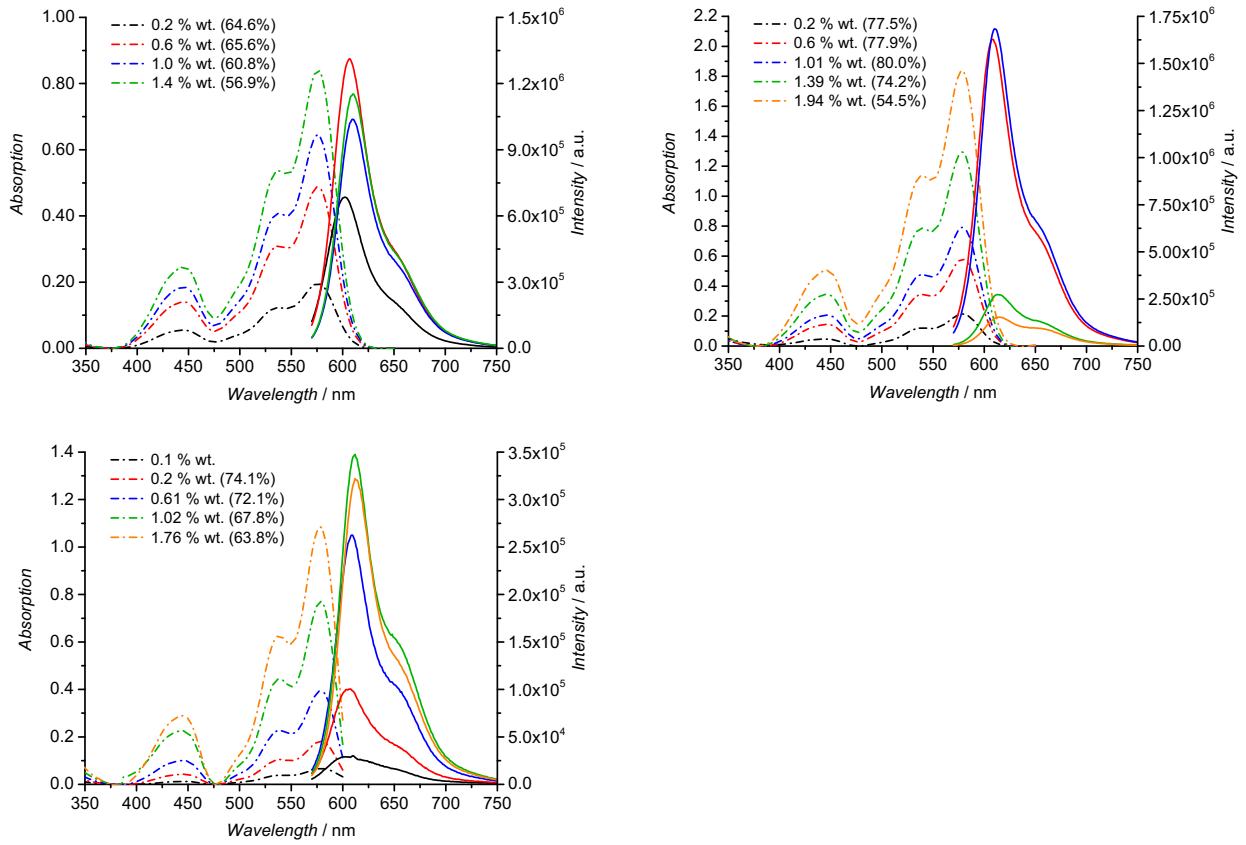

Figure 3. UV-vis absorption (dashed lines) and emission (solid lines) spectra of (a) LR/IGP2, (b) LR/GTP3, (c) LR/GTP4 films as a function of fluorophore concentration (wt.%). Excitation wavelength of 450 nm for all polymer films and absolute quantum yields reported in parentheses.

Conversely, LR/IGP2 films displayed emission features affected by fluorophore content (Figure 3a). When dispersed at low concentration in PMMA (i.e., 0.2-0.6 wt.%), LR showed a fluorescence emission peaked at 609 nm, respectively, with a Stokes shift of 39 nm, perfectly in agreement with results collected in PMMA.[22] Notably, LR is a strong emitter also in the solid phase with quantum yield (QY) higher than 70%. Above this range of concentration, the fluorescence band was affected by quenching phenomena like occurring in most of perylene-based fluorophores[22b] due to their aggregation-caused quenching (ACQ) character. The mild red-shift of the emission maximum probably originated from auto-absorption phenomena (inner filter effect). Nevertheless, LR

fluorescence in IGP2 was mostly retained with QY values of about 57% at the highest concentration (1.4 wt.%), thus making the films suitable for the preparation of LSCs. Identical results in terms of spectroscopic features were gathered from LR/IGP5 and are not reported and discussed for simplicity. As far as LR/GTP3 and LR/GTP4 films are concerned (Figure 3b and 3c), the optical features resulted mostly unchanged from the respective IGPn films in terms of absorption and emission wavelengths. Notably, similar to what observed for IGPn films, absorbance increased progressively with fluorophore content, whereas fluorescence quenching appeared less pronounced. It is worth noting that QY values of 74% was measured for LR/GTP3 containing the 1.4 wt.% of LR and of 64% for LR/GTP4 film with the highest fluorophore content of about 1.8 wt.%. These results are remarkable considering that the calculated QY of LR/PMMA films dropped from 86% to 69% by varying the fluorophore content from 0.2 to 1.4 wt.%. The higher emission efficiency of highly doped LR/GTPn films with respect to the corresponding LR/IGPn and LR/PMMA ones was possibly attributed to the presence of terephthalate units in the polymer composition. The aromatic content increases the matrix compatibility with the perylene-based core, thus limiting the ACQ behavior of LR. Moreover, the lower compatibilizing efficiency of the IGPn matrix could be also attributed to the low molecular weight (i.e., ~3000 g/mol compared to >20000 g/mol for GTPn) that possibly had a detrimental impact on the toughness of the derived thin films.

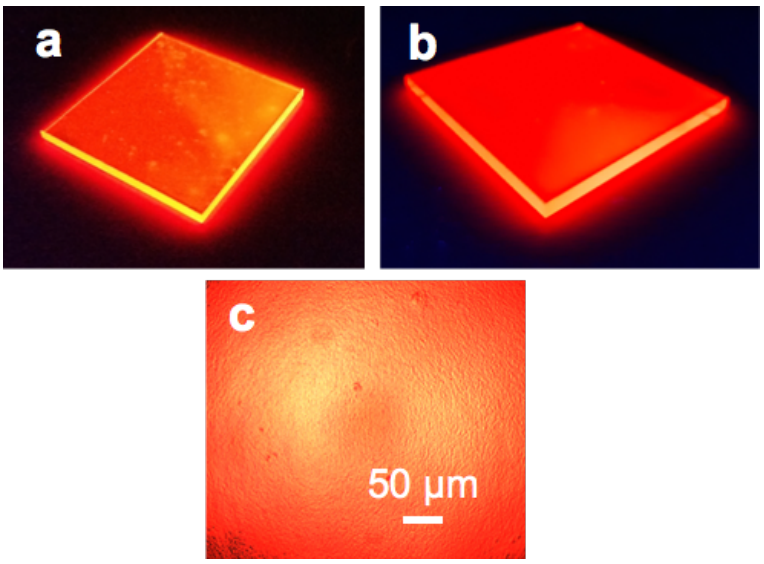

Figure 4. 5x5 mm 1.0 wt.% (a) LR/IPG2 and (b) LR/GTP3 films under the illumination of a Dark Reader Transilluminator at 450 nm and (c) optical microscopy image of the same LR/GTP3 sample

The emission of LR/IPG2 and LR/GTP3 films containing the 1 wt.% of fluorophore was also observed under the direct illumination at 450 nm (Figure 4a and 4b, respectively). In particular, the surface of the film based on IPG2 result less homogeneous with respect to that composed by GTP3. The very high compatibility between the GTP3 matrix and LR was corroborated by examining the film under an optical microscope. Negligible microphase-separation at the film surface was observed, thus confirming the suitability of the GTPn matrix for application in high performance LSC. In order to broaden the research also to another class of organic red-emissive molecules, LR was replaced with TPETPAFN, i.e. a highly conjugated aggregation-induced emission (AIE) fluorophore. AIE molecules (AIEgens) are non-fluorescent in solution of good solvents, but became highly emissive in poor solvents or in solid state, thus circumventing the adverse effects associated to the ACQ behavior also when dispersed in polymers.[23] In detail, TPETPAFN was designed to have high emission efficiency peaked at about 650 nm, high brightness in the aggregate state (QY = 42.5%) and strong photobleaching resistance.[24] GTP3 was selected as polymer matrix since it was demonstrated as compatible with highly conjugated aromatic fluorophores such as LR, thus possibly being suitable also for TPETPAFN.

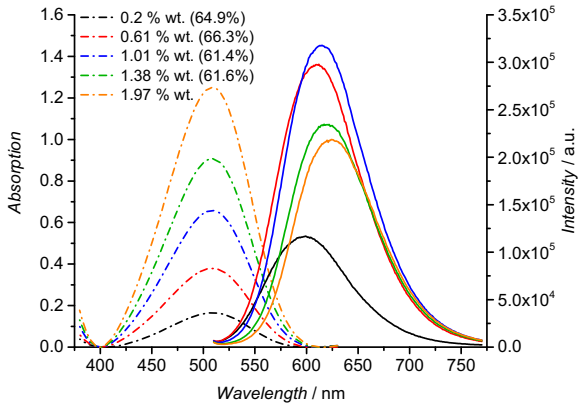

Figure 5. TPETPAFN/GTP3 films as a function of fluorophore concentration (wt.%). Excitation wavelength of 450 nm for all polymer films and absolute quantum yields reported in parentheses.

In Figure 5, the absorption and emission characteristics of TPETPAFN/GTP3 films are reported. TPETPAFN showed a broad molecular absorption peaked at about 500 nm, similarly to what observed in THF.[24] Notably, TPETPAFN/GTP3 films displayed a fluorescence emission peaked at

600-630 nm and with a very large Stokes shift higher than 100 nm. The emission intensity increased with the TPETPAFN content up to 1 wt.%, above which fluorescence quenching occurred, even if only partially. Indeed, profiting of the AIE features, the fluorescence QY resulted almost similar for all TPETPAFN/GTP3 films and never below 61% even at the highest fluorophore concentration investigated (i.e., 1.4 wt.%). In addition, a progressive red-shift of the emission maxima occurred with TPETPAFN content and possibly caused to auto-absorption phenomena (inner filter effect).[19c, 25] Moreover, the TPETPAFN/GTP3 film with the 1 wt.% of the AIE fluorophore showed excellent compatibility without any microphase separation (Figure S7). This results is noteworthy and strongly supports the use of the GTPn matrix in the realization of LSC based on renewable polymer matrices.

Optically efficiency determination of the prepared LSCs

The LSCs performances were determined by covering an optically pure 50 x 50 x 3 mm glass with the fluorophore-doped polymer films with a thickness of 25±5 μm. Photocurrent measurements were carried out with a home-built device based on a Si-based PV cell attached to one edge of the concentrator (see experimental section and Figures S8 and S9). The optical efficiency η_{opt} (Table 3) was calculated from the concentration factor C, which is the ratio between the short circuit current measured in the case of the cell over the LSC edge (I_{LSC}) and short circuit current of the bare cell when perpendicular to the light source (I_{SC}) (Eq. 1):

$$\eta_{opt} = \frac{I_{LSC}}{I_{SC} \cdot G} \text{ (eq. 1)},$$

where G is the geometrical factor (G = 16.6), which is the ratio between the area exposed to the light source and the collecting area.

Table 3. Optical efficiencies (η_{opt}) calculated for the prepared LSCs with different fluorophore content (wt.%). η_{opt} was calculated from an average of 3 measurements. Standard deviation is 0.1% for all the values reported in the table. In italic, the highest η_{opt} per film type.

Entry	**Fluorophore content (wt.%)**	**η_{opt} (%)**
LR/IGP2	0.2	5.4
	0.6	6.3
	1.0	*6.5*
	1.4	6.4
LR/GTP3	0.2	6.0

	0.6	6.4
	1.0	6.8
	1.4	*7.7*
	2.0	6.9
LR/GTP4	0.2	3.9
	0.6	3.8
	1.0	4.6
	1.4	5.0
TPETPAFN/GTP3	0.2	5.1
	0.6	5.8
	1.0	6.4
	1.4	*7.1*
	2.0	6.8
LR/PMMA	0.2	5.2
	0.6	6.0
	1.0	6.0
	1.4	*7.4*
	2.0	6.7

A similar trend of η_{opt} was found for all films. The optical efficiency increased as a function of dye concentration up to a certain content, after which it decreased slightly. This behavior originated in response to two opposing factors. Firstly, increasing the dye concentration increases the amount of emissive fluorophores in the film, thus potentially enhancing the solar harvesting efficiency. Secondly, dissipative phenomena such as re-absorption and fluorescent quenching, adversely affect the LSC performances. Notably, this behavior was also reflected to the QY variations with fluorophore concentrations (Figures 3 and 4). Especially at higher concentrations, these adverse effects become so significant that they counterbalance the beneficial effect of fluorophore contents. This explains why an optimal dye concentration was found for all films corresponding to about 1.4 wt.%. Furthermore, the highest optical efficiency of 7.7% was recorded for LR containing films based on GTP3, i.e. the polymer matrix already reported as the most promising for LSC being the most compatible with both fluorophores. It was worth noting that the value of 7.7% was higher than that of 7.4% gathered from the state of the art LR/PMMA thin films. These striking results definitely support the bio-based polyesters as renewable matrices for high performance LSCs. Moreover, the η_{opt} of 7.1% obtained from TPETPAFN/GTP3 films indicates that the proposed polymer matrix works well with both ACQ and AIE fluorophores.

4. Conclusions

This work demonstrated the potential of replacing state-of-the-art PMMA in LSC systems with renewable bio-based polyesters. Two types of polymers were synthesized, one from equimolar amounts of GxMe and isosorbide (IGPn), one from GxMe, terephthalate and 1,3-propanediol (GTPn) with feed molar composition of 0.25/0.25/0.5, respectively. All polymers showed the required thermal properties (Tg > 45 °C), transparency and stability to be used as host matrix in LSCs. GTPn copolymers showed to be highly compatible with LR and TPETPAFN fluorophores and provided thin films more homogeneous with respect to those based on IGPn. The higher compatibility possibly provided by the terephthalate units of GTPn and the higher molecular weight (M_w > 20000 g/mol compared to ~3000 g/mol of IGPn) conferred optical properties similar or superior to those collected from LR/PMMA thin films in the same range of fluorophore content. This feature was also reflected on the LSC performances, with maximum η_{opt} of 7.7% gathered from LR/GTP3 films, i.e. higher than that of 7.4% obtained from PMMA-based LSCs. These properties were also confirmed by using the AIE fluorophore TPETPAFN, thus definitely promoting the bio-based polyesters as renewable matrices for high performance LSCs.

Aknowledgements

The research leading to these results has received funding from the University of Pisa under PRA 2017 (project No. 2017_28) and BIHO 2017. We would like to thank Royal Cosun BV, the Netherlands, for providing us with the sugar-based monomers employed in this research and for the very fruitful discussions on the polymer synthesis. We also acknowledge AIEgen Biotech Co., Limited for the kind gift of a sample of TPETPAFN.

References

[1] M. A. Khan, M. Z. Khan, K. Zaman, L. Naz, *Renewable and Sustainable Energy Reviews* **2014**, *29*, 336-344; J. L. Sawin, in *Renewable Energy Policy Network for the 21th Century, Vol. 2014 Update*, Paris, **2014**.

[2] Y. Geng, W. Chen, Z. Liu, A. S. Chiu, W. Han, Z. Liu, S. Zhong, Y. Qian, W. You, X. Cui, *Journal of cleaner production* **2017**, *159*, 301-316.
[3] R. Judkoff, *MRS bulletin* **2008**, *33*, 449-454.
[4] N. Kampelis, K. Gobakis, V. Vagias, D. Kolokotsa, L. Standardi, D. Isidori, C. Cristalli, F. Montagnino, F. Paredes, P. Muratore, *Energy and Buildings* **2017**, *148*, 58-73.
[5] E. Recast, *Official Journal of the European Union* **2010**, *18*, 2010; E. Commissie, *Europese Commissie, Brussel* **2011**; M. Kanellakis, G. Martinopoulos, T. Zachariadis, *Energy Policy* **2013**, *62*, 1020-1030.
[6] N. Armaroli, V. Balzani, *Chemistry – A European Journal* **2016**, *22*, 32-57.
[7] F. Meinardi, F. Bruni, S. Brovelli, *Nature Reviews Materials* **2017**, *2*, 17072.
[8] M. G. Debije, P. P. C. Verbunt, *Advanced Energy Materials* **2012**, *2*, 12-35; M. Debije, *Nature* **2015**, *519*, 298-299; B. McKenna, R. C. Evans, *Advanced Materials* **2017**, *29*, 1606491.
[9] A. Goetzberger, W. Greube, *Applied physics* **1977**, *14*, 123-139.
[10] W. Van Sark, in *EPJ Web of Conferences, Vol. 33*, EDP Sciences, **2012**, p. 02003; W. G. Van Sark, K. W. Barnham, L. H. Slooff, A. J. Chatten, A. Büchtemann, A. Meyer, S. J. McCormack, R. Koole, D. J. Farrell, R. Bose, *Optics Express* **2008**, *16*, 21773-21792.
[11] M. D. Hughes, D.-A. Borca-Tasciuc, D. A. Kaminski, *Solar Energy Materials and Solar Cells* **2017**, *171*, 293-301; L. H. Slooff, E. E. Bende, A. R. Burgers, T. Budel, M. Pravettoni, R. P. Kenny, E. D. Dunlop, A. Büchtemann, *physica status solidi (RRL)–Rapid Research Letters* **2008**, *2*, 257-259.
[12] Y. Li, X. Zhang, Y. Zhang, R. Dong, C. K. Luscombe, *Journal of Polymer Science Part A: Polymer Chemistry* **2018**, *0*.
[13] R. P. Babu, K. O'Connor, R. Seeram, *Progress in biomaterials* **2013**, *2*, 8-8.
[14] V. Fattori, M. Melucci, L. Ferrante, M. Zambianchi, I. Manet, W. Oberhauser, G. Giambastiani, M. Frediani, G. Giachi, N. Camaioni, *Energy & Environmental Science* **2011**, *4*, 2849-2853; F. I. Chowdhury, C. Dick, L. Meng, S. M. Mahpeykar, B. Ahvazi, X. Wang, *RSC Advances* **2017**, *7*, 32436-32441.
[15] A. Gandini, *Polymer Chemistry* **2010**, *1*, 245-251.
[16] F. Fenouillot, A. Rousseau, G. Colomines, R. Saint-Loup, J. P. Pascault, *Progress in Polymer Science* **2010**, *35*, 578-622; E. de Jong, M. A. Dam, L. Sipos, G. J. M. Gruter, in *Biobased Monomers, Polymers, and Materials, Vol. 1105*, American Chemical Society, **2012**, pp. 1-13.
[17] I. Gavrila, P. Raffa, F. Picchioni, *Polymers* **2018**, *10*.
[18] B. Liu, A. Pucci, T. Baumgartner, *Materials Chemistry Frontiers* **2017**, *1*, 1689-1690.
[19] A. Pucci, *Israel Journal of Chemistry* **2018**, *58*, 837-844; R. Mori, G. Iasilli, M. Lessi, A. B. Munoz-Garcia, M. Pavone, F. Bellina, A. Pucci, *Polymer Chemistry* **2018**, *9*, 1168-1177; F. De Nisi, R. Francischello, A. Battisti, A. Panniello, E. Fanizza, M. Striccoli, X. Gu, N. L. C. Leung, B. Z. Tang, A. Pucci, *Materials Chemistry Frontiers* **2017**; J. L. Banal, B. Zhang, D. J. Jones, K. P. Ghiggino, W. W. H. Wong, *Acc. Chem. Res.* **2017**, *50*, 49-57.
[20] F. Gianfaldoni, F. De Nisi, G. Iasilli, A. Panniello, E. Fanizza, M. Striccoli, D. Ryuse, M. Shimizu, T. Biver, A. Pucci, *RSC Adv.* **2017**, *7*, 37302-37309.
[21] B. A. Noordover, V. G. van Staalduinen, R. Duchateau, C. E. Koning, R. A. van Benthem, M. Mak, A. Heise, A. E. Frissen, J. van Haveren, *Biomacromolecules* **2006**, *7*, 3406-3416.
[22] M. Carlotti, G. Ruggeri, F. Bellina, A. Pucci, *Journal of Luminescence* **2016**, *171*, 215-220; M. Carlotti, E. Fanizza, A. Panniello, A. Pucci, *Solar Energy* **2015**, *119*, 452-460.
[23] J. Mei, Y. Hong, J. W. Y. Lam, A. Qin, Y. Tang, B. Z. Tang, *Advanced Materials* **2014**, *26*, 5429-5479; J. Mei, N. L. C. Leung, R. T. K. Kwok, J. W. Y. Lam, B. Z. Tang, *Chemical Reviews* **2015**, *115*, 11718-11940.
[24] K. Li, W. Qin, D. Ding, N. Tomczak, J. Geng, R. Liu, J. Liu, X. Zhang, H. Liu, B. Liu, *Scientific reports* **2013**, *3*, 1150.
[25] J. Lucarelli, M. Lessi, C. Manzini, P. Minei, F. Bellina, A. Pucci, *Dyes and Pigments* **2016**, *135*, 154-162.